

**GEOLOGIC MAP
OF THE
TOLSTOJ (H-8)
QUADRANGLE
OF MERCURY**

By
Gerald G. Schaber and John F. McCauley

1980

Prepared for the
National Aeronautics and Space Administration
by
U.S. Department of the Interior, U.S. Geological Survey

(Published in hardcopy as USGS Miscellaneous Investigations Series Map I-1199, as part of the Atlas of Mercury, 1:5,000,000 Geologic Series. Hardcopy is available for sale from U.S. Geological Survey, Information Services, Box 25286, Federal Center, Denver, CO 80225)

Please direct questions or comments about the digital version to:
Richard Kozak
U.S. Geological Survey
2255 N. Gemini Drive
Flagstaff, AZ 86001
e-mail: rkozak@flagmail.wr.usgs.gov

DESCRIPTION OF MAP UNITS

PLAINS MATERIALS

- pvs VERY SMOOTH PLAINS MATERIAL—Occurs as smooth planar surfaces only in floors of c_4 and c_5 craters (FDS 529126). Very few superposed craters at Mariner 10 resolutions. *Interpretation:* Probably shock-melt and fallback associated with formation of individual craters
- ps SMOOTH PLAINS MATERIAL—Forms flat to gently rolling plains in extremely large annulus surrounding Caloris Basin, and in southeastern part of quadrangle in smaller patches associated with basin (for example, Tolstoj; FDS 166912) and crater (c_1 to c_3) floors (FDS 223). Also occurs in southeast in vague topographic lows of uncertain origin. Characterized by abundant small bright-halo craters (FDS 214, 221) and sharp overlapping contacts with older terrain. Sinuous to lobate ridges are abundant. *Interpretation:* Uncertain; some areas may consist of fluidized shock-melt materials created by Caloris impact. Alternatively, may be post-Caloris volcanic flows. Unequivocal volcanic vents and lava-flow fronts not observed. Unit appears to be equivalent to and younger than a late c_3 crater age, as indicated by relatively few superposed c_3 craters >30 km in diameter
- psi INTERMEDIATE PLAINS MATERIAL—Forms flat to rolling plains in c_1 to c_3 craters and in topographic depressions. Contains fewer superposed craters than intercrater plains but may form more convex, overlapping contacts with older terrain than do smooth plains (see craters Goya and Rublev: FDS 166907, 246, 223). *Interpretation:* Uncertain; may consist of shock-melt and breccia materials moved into topographic depressions by mass-wasting processes; may also consist in part of volcanic materials. Age relations to intercrater and smooth plains uncertain, primarily because of insufficient resolution. May have origin similar to smooth plains but deposited over a considerably longer period. Possibly analogous to widespread light lunar plains
- pi INTERCRATER PLAINS MATERIAL—Forms very extensive, gently rolling ground between large c_1 and c_2 craters, primarily in southeast half of quadrangle (FDS 124). Overlaps parts of Tolstoj Basin. Unit has high density of superposed 5- to 10-km-diameter craters, many of which are elongate and shallow or open on one side, features suggesting secondary-crater morphology (FDS 223). Surface nearly saturated with visually indistinct but topographically distinct circular depressions but essentially free of well-defined craters larger than about 50 km in diameter. *Interpretation:* A generally planar surface consisting of highly eroded remnants of large craters and basins that are only very shallow circular depressions (Malin, 1976). May consist of mixture of basin-related ejecta (breccia) and volcanic deposits emplaced during later stages of heavy bombardment (Strom, 1977). Embayment and transection relations of intercrater plains to craters and basins (for example, Tolstoj) suggest a complex history of contemporaneous formation
- cfp CALORIS FLOOR PLAINS MATERIAL—Closely resembles very smooth plains material (unit pvs) but exhibits more intense secondary deformation (FDS 106, 110, 195, 229). Sinuous ridges cut by tension fractures form grossly polygonal pattern dominated by two major trends, one concentric with respect to border of basin and the other

radial. Intensity of deformation appears to increase from basin rim inward. Surface of unit slopes toward center of basin floor (Hapke and others, 1975). *Interpretation:* Uncertain; probably post-Caloris volcanic flow materials, although unit could in part be shock-melt material associated with Caloris impact. Ridges and fractures suggest basin floor subsidence (ridge formation) followed by possible slight uplift forming tension fractures (Strom and others, 1975)

BASIN MATERIALS

CALORIS GROUP

- cm Caloris Montes Formation—Consists of numerous rectilinear massifs 1 to 2 km high and about 10 to 50 km long, mostly elongate radially from center of basin and separated by hackly-floored, radial troughs and gougelike structures. Surfaces of massifs are hackly. Best developed along inner edge of basin where steep inward-facing scarps are common, grading outward into smaller massifs and blocks. Marks crest of most prominent ring structure around Caloris. Type area: region near 18°, 184.5° (FDS 229) (McCauley and others, 1980). *Interpretation:* Uplifted prebasin bedrock covered by deep-seated late ejecta from Caloris. Inner boundary is approximate outer limit of crater of excavation
- cn Nervo Formation—Consists of patches of hackly to rolling plains that lie above both Caloris floor plains (unit cfp) and smooth plains surrounding Caloris Basin. Locally appears to be draped over subjacent blocks and massifs of the Caloris Montes Formation (unit cm). Type area: region in Shakespeare quadrangle near 40°, 177.5° (FDS 193) and south of unrelated crater Nervo (McCauley and others, 1980). *Interpretation:* Probably fallback mixed with impact melt
- co Odin Formation—Patches of hummocky plains that generally lie beyond major Caloris Montes scarp for as much as 1000 km. Consists of closely spaced to isolated smooth hummocks, usually 1 to 2 km across, separated by smooth plains; these plains resemble unit ps but for mapping convenience are included in this unit. Locally, hills are concentric with Caloris scarps. Type area: region around 25°, 170° (FDS 191, 72) (McCauley and others, 1980). *Interpretation:* Ejecta from Caloris embayed by smooth plains material. Individual hummocks and hills may represent coherent blocks of material from deeper parts of basin below mercurian megaregolith
- com Odin Formation (Mantling Preexisting Terrain)—Extensive patches of hummocky deposits that mantle preexisting crater and plains units as far as 1200 km beyond edge of Caloris Basin. Consists of closely spaced, rounded hummocks usually 3 to 8 km across, separated by smoother plains that resemble units pi and psi. Preexisting topography apparent. Type area: region around -2.5°, 170° (FDS 56, 63). *Interpretation:* Ejecta from Caloris; individual hummocks and hills may represent coherent blocks of material from deeper parts of basin. Most contacts of unit farthest from Caloris with intercrater plains (unit pi) and c₁ and c₂ crater materials difficult to map with confidence
- cvl Van Eyck Formation, Lineated Facies—Scattered outward from about limit of weak outer Caloris scarp for distance of about 1000 km. Forms long, wavy radial ridges and intervening grooves. Some ridges sharply bounded by scarps. Extensively embayed by smooth plains material (unit ps). Type area: southwest edge of Van Eyck Basin in Shakespeare

quadrangle near 40°, 163° (FDS 189) (McCauley and others, 1980). *Interpretation:* Ejecta from Caloris and radial structures formed by Caloris event. Secondary cratering played important role in development of surface morphology. Most grooves are probably buried secondaries. Ejecta from shallower layers in pre-Caloris surface than those that were source of other formations in Caloris Group

- cvs Van Eyck Formation, Secondary-Crater Facies—Consists of chains and clusters of craters that are generally superposed on cratered terrain in southeast but are also locally gradational with distal ends of lineated facies (unit cvl). Degree of freshness uniform except near large younger craters. Type area: crater cluster on rim of crater Po Chu-I at -7°, 166° (FDS 0529131) (McCauley and others, 1980). *Interpretation:* Far-flung secondaries from Caloris that lie within and beyond limit of thin, discontinuous part of ejecta blanket. These secondaries were little affected by later arriving ejecta and other secondaries, as was lineated facies of the Van Eyck
- trl TOLSTOJ BASIN RIM MATERIAL—Rises slightly above intercrater plains. Characterized by radial lineations and grooves. Rectilinear map pattern. Pronounced dark albedo between inner and outer rings of basin. Type area: regions around -10°, 153° (FDS 246) and -21°, 171° (FDS 166912). *Interpretation:* Radially lineated and grooved rim ejecta from Tolstoj Basin, consisting of shock breccia and shock-melt materials derived from depth. Lineations and grooves represent secondary-crater scour and in part post-depositional structural deformation. Rectilinear map pattern of unit discussed in text. Dark albedo of some materials probably compositional (Hapke and others, 1975). Overlap of intercrater plains (unit pi) onto northwest side of Tolstoj suggests that basin impact was an early pi event

CRATER MATERIALS

CRATER MATERIALS—Craters >30 km in diameter

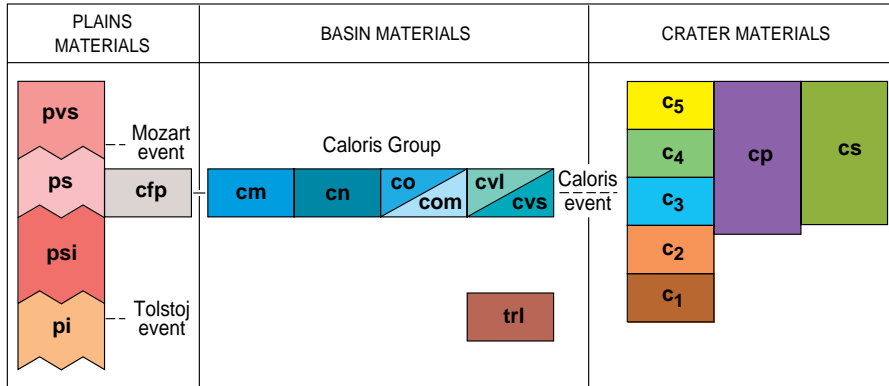
- c5 Material with very fresh appearing, sharp rims, wall terraces, and central peaks (FDS 121, 126, 529126). Well-defined, continuous fields of relatively sharp secondary-crater clusters and chains, of which only the larger are mapped (sc). Sharp break between wall and floor materials. Floors generally filled with very smooth plains material (unit pvs)
- c4 Material with prominent, continuous, only slightly subdued rims, wall terraces, and central peaks (FDS 116, 166827). Most floors partly filled with very smooth plains materials (unit pvs). Break at base of wall still distinct. Floor and wall contact not visible in crater Mozart. Well-preserved, extensive secondary-crater fields; low number of superposed craters
- c3 Material with low, rounded, but continuous rims and with flat floors generally filled with intermediate plains and smooth plains materials (units psi and ps) (FDS 222, 166912). Floor-wall boundary indistinct in many craters. No well-defined secondary-crater fields surround craters <100 km across. Craters >100 km in diameter have discontinuous, only partly preserved secondaries. Moderate number of superposed craters
- c2 Material with a pan-shaped profile and with low, greatly subdued, continuous to discontinuous rims (FDS 166912, 166913). No wall terraces, rare central peaks. Crater floor generally filled with

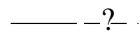
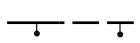



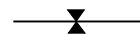






intermediate plains and smooth plains materials (units psi and ps). Floor-wall boundary very indistinct. No visible secondaries; many superposed craters

- c1 Material of flat-floored craters with extremely low and discontinuous rims rising only slightly above intercrater plains. Rare central peaks; wall structure and satellite craters are absent (FDS 62, 124, 215). Most craters >100 km in diameter, many filled with intermediate plains and smooth plains materials (units psi and ps) *Interpretation:* Impact craters displaying various degrees of degradation and infilling; state of degradation can be misleading age criterion because of proximity of crater to younger impact craters and associated secondary-crater effects that are more intense near a primary on Mercury than on the Moon. Morphologic classification of mercurian craters <100 km and >100 km in diameter has been described by N. J. Trask (fig. 10 in McCauley and others, 1980)
- cp CENTRAL PEAK MATERIAL—Occurs in c2 to c5 craters as single hills or small semicircular clusters of hills rising above crater floors near their centers (FDS 116, 529126). *Interpretation:* Precrater brecciated rocks uplifted and deformed at time of impact
- cs SECONDARY CRATER MATERIAL—Occurs as chains and clusters of moderately fresh to subdued craters, many relatable to nearby primary craters. *Interpretation:* Near- and far-flung secondary ejecta from primary impacts. Only larger secondary-crater chains and clusters from each crater and basin are mapped (for example, crater Mozart)

NOTE The area shown as geologic unit cv1 (Caloris Group—Van Eyck Formation) centered at lat. 23° N. and long. 162°, should be unit com (Odin Formation mantling preexisting terrain). The preexisting terrain at this locality is considered to be ejecta rim deposits from an unnamed 355-km-diameter basin centered at lat. 28° N, and long. 158.5°, in the Shakespeare quadrangle (H-3).

CORRELATION OF MAP UNITS



	Contact—Queried where doubtful
	Scarp, probably a fault—Dashed where subdued. Bar and ball on downthrown side
	Lineament—Probably a fault with no vertical relief or uncertain displacement. May include unresolved crater chains of secondary-impact origin
	Narrow to broad ridge—Interpreted within units cvl and co and plains materials (units pi, ps, and cfp) as mare-type wrinkle ridge due to shrinkage. Symbol on ridge crest
	Ridge scarp, linear to arcuate—Interpreted within units co and com and plains materials (units psi, ps, and cfp) as edge of mare-type wrinkle ridge. Line marks base of slope; barb points downslope
	Fissure or depression of structural origin, linear to arcuate—Restricted to unit cfp in floor of Caloris Basin. Barbs point downslope
	Scarp, linear to arcuate—Interpreted as fault scarp or depression of structural or erosional origin
	Crater rim crest
	Crater rim crest—Greatly subdued or buried
	Crestline of concentric rings surrounding Caloris and Tolstoj Basins—Interpreted as structural ring fractures formed during and immediately after these impacts
	Area of bright crater-ray material—Interpreted as ejecta from very fresh impacts
	Area of abnormally low albedo

INTRODUCTION

The Tolstoj quadrangle in the equatorial region of Mercury contains the southern part of Caloris Planitia, which is the largest and best preserved basin seen by Mariner 10. This basin, about 1300 km in diameter, is surrounded by a discontinuous annulus of ejecta deposits of the Caloris Group (units cm, cn, co, cvl, and cvs) that are embayed and covered by broad expanses of smooth plains (unit ps). The southeast half of the quadrangle is dominated by ancient crater deposits (units c₁, c₂, and c₃), by nondescript rolling to hummocky plains materials (unit pi) between individual craters, and by isolated patches of nondescript plains (units pi-ps). The ancient and degraded Tolstoj multiring basin, about 350 km in diameter, is in the south-central part of the quadrangle. The large, well-preserved crater Mozart (285 km diameter) is a prominent feature in the western part of the area; its extensive ejecta blanket and secondary crater field are superposed on the smooth plains (unit ps) surrounding Caloris.

Low-albedo features Solitudo Neptunii and Solitudo Helii, adopted from telescopic mapping, appear to be associated with the smooth plains material (unit ps) surrounding Caloris; a third low-albedo feature, Solitudo Maiiae, appears to be associated with the Tolstoj Basin. (For location of albedo features see Davies and others, 1978, p. 15.)

Mercury's rotation period of 58.64 days is in two-thirds resonance with its orbital period of 87.97 days. Therefore, at its equator, longitudes 0° and 180° are subsolar points ("hot poles") near alternate perihelion passage (Davies and others, 1978). The "hot pole" at 180° lies within the Tolstoj quadrangle; at perihelion, equatorial temperatures range from about 100° K at local midnight to 700° K at local noon. This daily range of 600° K is greater than that on any other body in the solar system (Davies and others, 1978).

Mariner 10 photographic coverage was available for only the eastern two-thirds of the Tolstoj quadrangle. Image data from three Mariner 10 encounters with Mercury were used in mapping the quadrangle.

STRATIGRAPHY

OLDER PLAINS MATERIALS

The rolling to hummocky plains that lie between large craters in the southeastern part of the quadrangle make up the oldest recognizable map unit, the intercrater plains material (unit pi). The plains were originally described as intercrater by Trask and Guest (1975), who noted their level to gently rolling appearance and their general lack of well-defined craters larger than about 50 km in diameter. Malin (1976) showed the plains to contain highly eroded remnants of large craters and basins that are only very shallow circular depressions. These intercrater plains are, however, marked by a very high density of superposed craters that are small (5-10 km diameter), elongate, shallow, and probably secondary to the many large craters superposed on the plains. Superposition of crater ejecta over parts of intercrater plains in other areas indicates that some large craters formed in a preexisting intercrater plains unit. On the other hand, the intercrater plains material partly postdates some of the major cratering events on Mercury, according to apparent superposition relations (Malin, 1976; Guest and O'Donnell, 1977). In particular, the unit appears to overlap the entire northwest side of the Tolstoj Basin, a feature indicating that the intercrater plains in this region probably do not represent the remains of the primordial surface of the planet. A complex history of contemporaneous craters and plains formation is therefore suggested. A detailed discussion of the origin of the intercrater plains on the Moon and Mercury was given by Strom (1977).

Patches of less cratered, smoother, less rolling plains occur throughout the quadrangle, but their recognition is highly dependent on the resolution and lighting of individual Mariner 10 frames. Therefore, because their distribution cannot now be mapped accurately, many of these patches are included with the smooth plains material (unit ps). Certain patches of these intermediate plains, where clearly rougher and possibly older than unit ps, are mapped as the intermediate plains material (unit psi). These patches occur mostly within the floors of c₁, c₂, and c₃ craters and are distinguished by a slightly greater density of small craters and a lower incidence of small bright-halo craters than are found on the smooth plains material (unit ps). The presence of plains intermediate in roughness and crater density between the oldest plains (unit pi) and the post-Caloris plains (unit ps) suggests that plains formation was a more or less continuous process that spanned much of the early geologic history of Mercury.

BASIN MATERIALS

The impact that produced the Tolstoj Basin occurred very early in the history of the quadrangle. Two ragged, discontinuous rings approximately 356 km and 510 km in diameter encompass the structure but are poorly developed on its north and northeast sides; a third partial ring with a diameter of 466 km occurs on its southeast side. Diffuse patches of material of dark albedo lie outside the innermost ring. The central part of the basin is covered by smooth plains material (unit ps). Hapke and others (1975) have suggested that the dark-albedo materials associated with the Tolstoj Basin margins are distinctly bluer than the surrounding terrain, whereas the plains filling the interior are distinctly redder.

Despite Tolstoj's great age and its embayment by the ancient inter-crater plains, it retains an extensive and remarkably well preserved, radially lineated ejecta blanket (unit trl) around two-thirds of its circumference. The ejecta tends to be blocky and only weakly lineated between the inner and outer rings. Radial lineations with a slight swirly pattern are best seen on the southwest side of Tolstoj. The unusual rectilinear map pattern of the ejecta suggests: (1) control of the ejecta pattern by prebasin structures, (2) preferential burial along structural trends of an originally symmetrical ejecta blanket by the intercrater plains material (unit pi), or (3) formation of Tolstoj by an oblique impact from the northwest that produced an ejecta blanket with bilateral symmetry and little or no deposition uprange. Analysis of stereo-photography of Tolstoj ejecta northeast of the crater suggests that this deposit has been upwarped to a higher elevation relative to the surrounding plains.

Caloris Group

The Caloris Basin is especially significant from a stratigraphic standpoint. Like the Imbrium and Orientale Basins on the Moon, it is surrounded by an extensive and well-preserved ejecta blanket (Strom and others, 1975; Trask and Guest, 1975; Guest and O'Donnell, 1977). As on the Moon, where ejecta from the better preserved basins was used to construct a stratigraphy, the ejecta from the Caloris Basin also can be used as a marker horizon. This ejecta is recognizable to a distance of about one basin diameter in the Tolstoj quadrangle and the adjacent Shakespeare quadrangle to the north. Undoubtedly, the ejecta also influences a large part of the as-yet-unseen terrain to the west. A stratigraphic and structural comparison between the Orientale and Caloris Basins has been made by McCauley (1977). McCauley and others (1980) have proposed a formal rock stratigraphy for the Caloris Basin that we have adopted on the present map. This stratigraphy is patterned after that used in and around the Orientale Basin on the Moon (Scott and others, 1977) and should aid in the future recognition of pre- and post-Caloris events over a broad expanse of the surface of Mercury. Crater degradation chronologies, such as the one modified from Trask (McCauley and others, 1980), and correlations between

plains units on the basis of crater frequency may aid in tying much of the remainder of the surface of Mercury to the Caloris event.

Unlike the Imbrium-related stratigraphy of Shoemaker and Hackman (1962), that devised for Mercury is a rock rather than a time stratigraphy. It recognizes the existence of an orderly, in essence isochronous sequence of mappable units around Caloris that are similar in character to those recognized around the better preserved impact basins of the Moon such as Orientale, Imbrium, and Nectaris.

McCauley and others (1980) have proposed the name "Caloris Group" to include the mappable units created by the impact that formed the Caloris Basin and have formally named four formations within the group, which were first recognized and named informally by Trask and Guest (1975). The formations are here described from the basin rim outward.

The Caloris Montes Formation (unit cm), which was informally called the Caloris mountains terrain by Trask and Guest (1975), consists of a jumbled array of smooth-appearing but highly segmented mountain massifs that rise 1-2 km above the surrounding terrain. These massifs mark the crestline of the most prominent scarp or ring of the Caloris Basin and grade outward into smaller blocks and lineated terrain. The Caloris Montes Formation is very similar in morphology to and is considered the equivalent of the massif facies of the Montes Rook Formation around the Orientale Basin (Scott and others, 1977; McCauley and others, 1980). The Caloris Montes is interpreted as basin rim deposits consisting of ejecta from deep within Caloris that is mixed with but generally overlies uplifted and highly fractured prebasin bedrock (McCauley, 1977).

The Nervo Formation (unit cn) consists of rolling to locally hummocky plains that lie in intermassif depressions. The plains generally lie within the annulus of rugged terrain marked by the Caloris Montes Formation and locally appear to drape and overlie some of the more low-lying massifs. The Nervo bears some resemblance to the Apennine Bench Formation around the Imbrium Basin (Hackman, 1966); its closest counterpart in Orientale is the knobby facies of the Montes Rook Formation (Scott and others, 1977). The Nervo Formation was originally designated the intermontane plains by Trask and Guest (1975) and has been interpreted by them as fallback ejecta, an interpretation that seems to explain its distribution pattern and relative roughness as well as the fact that it is generally perched above the smooth plains (unit ps) that encompass Caloris.

The Odin Formation (units co and com), which was originally called the hummocky plains by Trask and Guest (1975), was described by them as consisting of closely spaced, smooth hills about 1 km across. The area between the hills is similar in appearance to the smooth plains (unit ps), but for mapping convenience this area has been included in the Odin Formation. The distribution pattern of the Odin is highly dependent on resolution and lighting but in general appears similar to that of the Alpes Formation of the Imbrium Basin on the Moon. The Odin, like the Alpes, occurs in broad lobes (unit co) such as those in Odin Planitia beyond the main basin scarp. As unit com, the Odin also mantles the intercrater plains (unit pi) and c₁ and c₂ crater materials out to a distance of 1200 km from the main Caloris scarp. The Odin Formation is interpreted as part of the Caloris ejecta sequence, but its mode of origin is less clear than those of certain other Caloris formations. The unit may consist of late-arriving, blocky, coherent ejecta from deep within the Caloris cavity, later partly buried by smooth plains (unit ps).

The Van Eyck Formation (units cvl and cvs), which is the most distinctive of the circum-Caloris stratigraphic units, was called the Caloris lineated terrain by Trask and Guest (1975). The inner boundary of the Van Eyck is generally coincident with the weak outer Caloris scarp. The unit forms radial ridges and grooves that are extensively embayed by smooth plains (unit ps). The Van Eyck is similar in morphology but somewhat more degraded than the Fra Mauro Formation around the Imbrium Basin on the Moon; secondary cratering and ballistic deposition of

ejecta from Caloris undoubtedly played an important role in its emplacement. It is difficult to define individual secondary craters within the Van Eyck, but at a distance of about one basin diameter, numerous clusters and chains of moderately well preserved craters occur that are interpreted as far-flung Caloris secondary craters. These craters have been included in a separate facies (unit cvs) of the Van Eyck Formation because of their regional stratigraphic significance.

YOUNGER PLAINS MATERIALS

The Caloris floor plains material (unit cfp) is a special problem and is not included in the Caloris Group. The plains have some features in common with the Maunder Formation in the floor of Orientale on the Moon (McCauley, 1977; Scott and others, 1977) but do not show the radial and circumferential ridges characteristic of the Maunder that led to its interpretation as a basin floor unit. The Caloris floor plains have a more open, coarser fracture pattern than does the Maunder. In addition, the Caloris ridges and the fractures cutting them have a crude rhombic pattern that led Strom and others (1975) to conclude that the plains materials subsided and then were gently uplifted to produce the open tension fractures observed. The ridges in the floor of Caloris lack the crenulated crests that are common on lunar ridges. Regardless of the origin and tectonic history of these plains, it seems clear that they represent a deep basin fill that obscures the original floor of the Caloris Basin.

The largest single expanse of the smooth plains material (unit ps) surrounds the Caloris Basin—mostly in Tir and Budh Planitiae—but many smaller patches occur in crater floors and other topographic depressions within the heavily cratered terrain in the southeastern part of the quadrangle. The plains are characterized by a relatively sparse crater density and an abundance of mare-type wrinkle ridges; overlap relations indicate that the plains are younger than the more densely cratered units. The plains also embay the Caloris Formation and account in particular for the skeletal map pattern of the Van Eyck Formation (unit cvl). The ubiquitous distribution of unit ps in topographically low regions supports the hypothesis that these materials were deposited in a fluid or semifluid state as basin ejecta or volcanic flows. The plains are thought to be slightly younger but date to the same age as the Caloris Basin materials (Trask and Guest, 1975); thus parts of the plains are probably Caloris ejecta, either impact melt or very fluid debris flows. No obvious secondary craters from Caloris have been recognized on the smooth plains. The presence of large patches of smooth plains in the floor of the Tolstoj Basin and in irregular depressions in the extreme southeastern part of the map indicates that at least some of these materials may be volcanic (Schultz, 1977). However, the absence of unequivocal lava-flow fronts and well-defined volcanic vents such as those of the lunar maria prevents a firm conclusion regarding volcanic origin.

Small patches of very smooth plains material (unit pvs) occur in the floors of many of the youngest craters. The patches may consist of fallback and impact melt related to the formation of individual craters and therefore may not represent late-stage volcanic fill or volcanic modification of the more youthful mercurian craters. Schultz (1977) suggested compositional differences or endogenic modification as possible causes of the color contrasts among the floor, wall, and rim areas of the dark-halo craters Zeami (120 km diameter), Tyagaraja (100 km diameter), and Balzac (80 km diameter). The dark ejecta and floors plains of these craters are distinctly redder than the surrounding plains, whereas their anomalously bright floor patches, central peaks, and wall areas are distinctly bluer. None of these dark-halo craters has associated bright rays, although secondary craters are well preserved. Compositional implications of contrasting color differences for mercurian crater and plains materials have been discussed by Hapke and others (1975).

CRATER MATERIALS

The mapping employs a fivefold division of craters on the basis of their apparent freshness (McCauley and others, 1980); craters less than about 30 km diameter were not mapped. A random distribution of c_4 and c_5 craters occurs throughout the quadrangle, superposed on all other units. The Caloris event appears to have occurred late in c_3 time, and Tolstoj appears to be an early c_1 event (McCauley and others, 1980).

Cumulative crater-size frequency distribution curves for the smooth plains (unit ps) and heavily cratered terrain (units c_1 to c_5 and unit pi) are shown in figures 1 and 2. The plains have a crater density similar to that of the Cayley Plains Formation on the Moon and, if their cratering history is about the same, have a similar age (3.9 to 3.8 b.y.). Significant disagreement exists, however, concerning the cratering rate on Mercury relative to the Moon. The crater curves for the heavily cratered terrain (fig. 2) show a general superposition on the 10-percent saturation line (Gault, 1970) for crater diameters between 50 and 90 km, but a rapid falloff from this line below and above these extreme diameters. The relation of crater distribution between lunar and mercurian heavily cratered terrain was described by Strom (1977). Schaber and others (1977) discussed the reduction in numbers of craters and basins per unit area on Mercury relative to the Moon.

STRUCTURE

The circumbasin scarps around Caloris, Tolstoj, and Mozart are the most prominent structural features in the quadrangle. The main Caloris Montes scarp is thought to approximate the edge of the basin of excavation of Caloris and is probably a structural and stratigraphic counterpart of the Montes Rook scarp around the Orientale Basin on the Moon (McCauley, 1977). A subdued outer scarp is present around most of the visible part of Caloris, better seen in the Shakespeare quadrangle to the north. This scarp is generally coincident with the transition between the massifs of the Caloris Montes Formation (cm) and the lineated facies of the Van Eyck Formation (unit cvl). The roughly rectilinear outlines of massifs within the Caloris Montes suggest structural control by a prebasin fracture pattern. The much lower, discontinuous outer scarp is considered to be the feeble equivalent of the Montes Cordillera scarp around Orientale. Like the Cordillera, it probably lies outside the limit of the crater of excavation. Its poor development and spacing much closer to the edge of the basin may be due to the greater mercurian gravity, as described by Gault and others (1975). The Van Eyck Formation is characterized by an extensive radial ridge-and-valley system with minor concentric scarps and lineaments. These features are considered for the most part as gouges and depositional plumes from secondary cratering within the Van Eyck; the remarkably straight ridges and steep walls, however, suggest formation by fracturing.

Only a small part of the ridge and fracture system that characterizes the floor of Caloris is within the quadrangle. The ridges in the floor of Caloris, which are like those within the smooth plains (unit ps), do not appear to be as complex as lunar mare ridges and are cut by numerous open grabenlike gashes. This area and its antipode in the Discovery quadrangle are the only two on Mercury where tensional forces can now be seen to have shaped the surface (Strom and others, 1975).

The Tolstoj Basin is encompassed by parts of at least three ragged and discontinuous inward-facing scarps. Lineated ejecta is best developed in the vicinity of and beyond the outer scarp, whereas blocky materials occur between the inner and outer scarps. These relations are similar to those around Caloris, although Tolstoj is less than half its size and is much more severely degraded by later impact cratering.

The sharpness of the single rim-scarp of Mozart reflects the youth (younger than unit ps) of this large impact. The position of Mozart at the west terminator of the

Mariner 10 image data precludes visibility of its floor and thus hides any evidence of a possible central uplift or inner structural ring.

Lobate scarps or ridges, which are best seen within the smooth plains material (unit ps) and vary locally within the intercrater plains material (unit pi), are generally steep on one side and gently dipping on the other. Some, like the lunar mare ridges, appear to mark the outlines of subjacent craters. Most workers, particularly Strom and others (1975), Melosh (1977), and Melosh and Dzurisin (1978), have ascribed these ridges to compression and a slight shortening of the crust of Mercury after formation of most of the present surface. Some ridges, however, may represent flow fronts, but their estimated heights of several hundred meters would require formation by extraordinarily viscous lavas.

Numerous faint lineaments are visible within the quadrangle, especially in the area between the Tolstoj Basin and the large crater Zeami to the northeast (fig. 3). Many of these lineaments may be faint secondary-crater chains or gouges; others may represent traces of an ancestral structural pattern that partly controlled the excavation of the craters and basin. The lineaments may have been enhanced or preserved by the gentle upwarping of this region of Tolstoj ejecta discussed above. The largest lineament, which marks the northwest limit of recognizable Tolstoj ejecta, is a subdued scarp some 450 km long. Rejuvenation of earlier faults or fractures by subsequent impacts probably occurred throughout the history of the planet. Thus, except for the lobate compressional scarps, it is difficult to separate internally produced structures from those of the complex impact history of Mercury. The azimuthal trends of all lineaments mapped within the quadrangle are, however, dominantly northwest (315°) and northeast (35° – 40°) (fig. 3). A minor, almost north-south trend is also observed. This situation is reminiscent of the so-called lunar grid on the Moon, which is generally ascribed to planetwide internal causes.

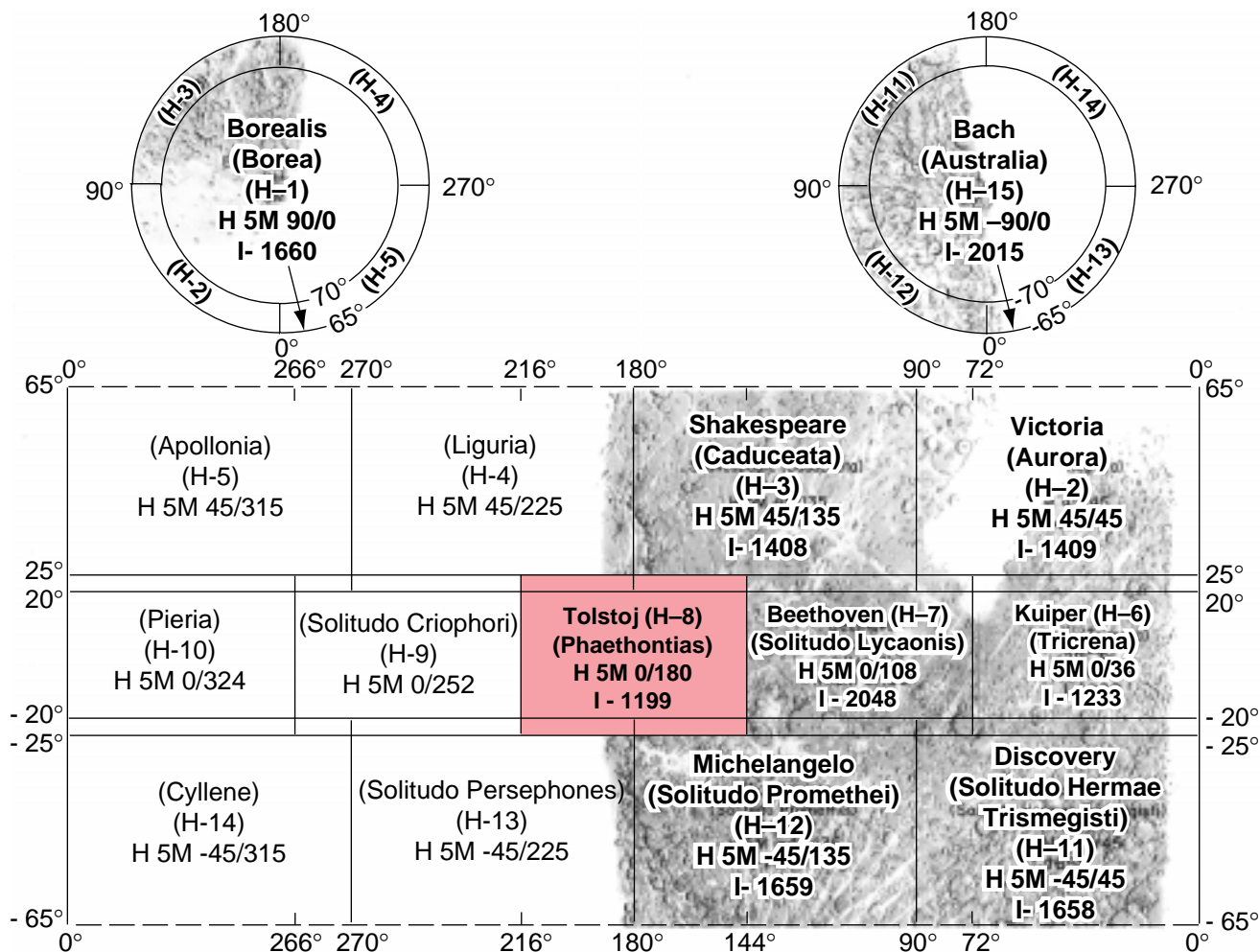
GEOLOGIC HISTORY

The interpretable geologic history within the Tolstoj quadrangle begins with the period of formation of the intercrater plains (unit pi), which persisted until shortly after impact of the asteroid that created the Tolstoj Basin. After this event was a period of only slightly less intense bombardment when the c_1 and largest c_2 craters were superposed on the intercrater plains. This period was followed by impact of the asteroid that created the Caloris Basin and deposits of the Caloris Group. Although the intermediate plains (unit psi) were resurfaced at the time of the Caloris impact, their formation actually extended from the end of the intercrater plains-forming period through the end of formation of c_3 craters. At about the time the last c_3 craters and the first c_4 craters were being formed, the upper surface of the smooth plains (unit ps) and Caloris floor plains (unit cfp) were being emplaced. Part of the smooth plains and Caloris floor plains materials may have been deposited during or immediately after the Caloris event.

After the emplacement of most of the smooth plains, some late c_3 craters and all c_4 and c_5 craters, including the large crater Mozart, were superposed on all previous deposits. The recognizable geologic history of the quadrangle ends with these events probably several billion years ago. A summary of the generalized geology history of Mercury was given by Guest and O'Donnell (1977) and Davies and others (1978).

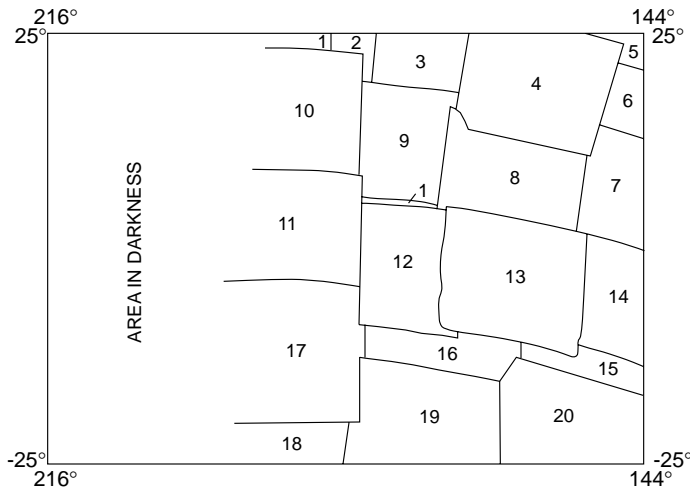
REFERENCES

- Davies, M. E., Dwornik, S. E., Gault, D. E., and Strom, R. G., 1978, Atlas of Mercury: National Aeronautics and Space Administration Special Publication SP-423, 128 p.
- Gault, D. E., 1970, Saturation and equilibrium conditions for impact cratering on the lunar surface: Criteria and implications: *Radio Science*, v. 5, no. 2, p. 273–291.
- Gault, D. E., Guest, J. E., Murray, J. B., Dzurisin, Daniel, and Malin, M. C., 1975, Some comparisons of impact craters on Mercury and the Moon: *Journal of Geophysical Research*, v. 80, no. 17, p. 2444–2460.
- Guest, J. E., and O'Donnell, W. P., 1977, Surface history of Mercury: A review: *Vistas in Astronomy*, v. 20, p. 273–300.
- Hackman, R. J., 1966, Geologic map of the Montes Apenninus region of the Moon: U.S. Geological Survey Miscellaneous Investigations Series Map I-463, scale 1:1,000,000.
- Hapke, Bruce, Danielson, G. E., Jr., Klaasen, Kenneth, and Wilson, Lionel, 1975, Photometric observations of Mercury from Mariner 10, 1975: *Journal of Geophysical Research* v. 80, no. 17, p. 2431–2443.
- McCauley, J. F., 1977, Orientale and Caloris: *Physics of the Earth and Planetary Interiors*, v. 15, no. 2–3, p. 220–250.
- McCauley, J. F., Guest, J. E., Schaber, G. G., Trask, N. J., and Greeley, Ronald, 1980, Stratigraphy of the Caloris Basin, Mercury: *Icarus*, (in press).
- Malin, M. C., 1976, Observations of intercrater plains on Mercury: *Geophysical Research Letter*, v. 3, no. 10, p. 581–584.
- Melosh, H. J., 1977, Global tectonics of a despun planet: *Icarus*, v. 31, p. 221–243.
- Melosh, H. J., and Dzurisin, Daniel, 1978, Mercurian global tectonics: A consequence of tidal despinning?: *Icarus*, v. 35, p. 227–236.
- Schaber, G. G., Boyce, J. M., and Trask, N. J., 1977, Moon-Mercury: Large impact structures, isostasy, and average crustal viscosity: *Physics of the Earth and Planetary Interiors*, v. 15, no. 2–3, p. 189–201.
- Schultz, P. H., 1977, Endogenic modification of impact craters on Mercury: *Physics of the Earth and Planetary Interiors*, v. 15, no. 2–3, p. 202–219.
- Scott, D. H., McCauley, J. F., and West, M. N., 1977, Geologic map of the west side of the Moon: U.S. Geological Survey Miscellaneous Investigations Series Map I-1034, scale 1:5,000,000.
- Shoemaker, E. M., and Hackman, R. J., 1962, Stratigraphic basis for a lunar time scale, in Kopal, Zdenek, and Mikhailov, Z. K., eds., *The Moon: International Astronomical Union Symposium, 14th, Leningrad, U.S.S.R., 1960*: London, Academic Press, p. 289–300.
- Strom, R. G., 1977, Origin and relative age of lunar and mercurian intercrater plains: *Physics of the Earth and Planetary Interiors*, v. 15, no. 2–3, p. 156–172.
- Strom, R. G., Trask, N. J., and Guest, J. E., 1975, Tectonism and volcanism on Mercury: *Journal of Geophysical Research*, v. 80, no. 17, p. 2478–2507.
- Trask, N. J., and Guest, J. E., 1975, Preliminary geologic terrain map of Mercury: *Journal of Geophysical Research*, v. 80, no. 17, p. 2461–2477.



ARRANGEMENT OF MAP SHEETS ON MERCURY

The provisional name "Goethe" was changed to "Borealis," and the provisional name "Tir" was changed to "Tolstoj" by the International Astronomical Union in 1976 (IAU, 1977). These provisional names appeared on earlier editions of this index map and on the shaded relief map of Tolstoj (H-8) quadrangle. The number preceded by I refers to published geologic map.

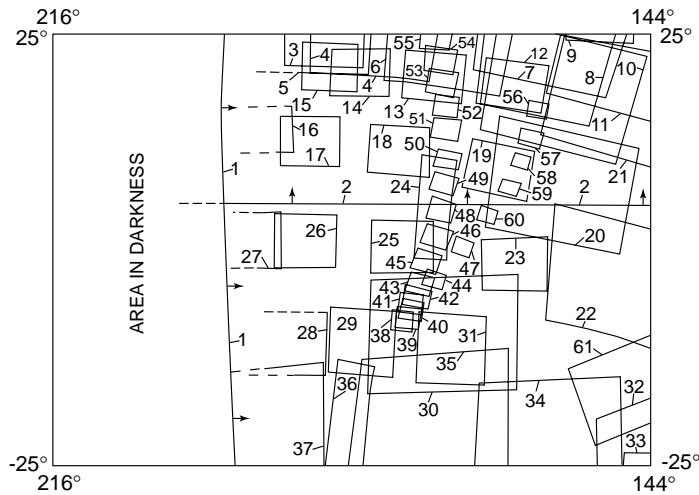


Index No. FDS No.

1	503
2	228
3	225
4	221
5	182
6	183
7	214
8	222
9	226
10	229
11	230
12	227
13	223
14	219
15	246
16	244
17	231
18	310
19	240
20	242

INDEX TO MARINER 10 PICTURES

The mosaic used to control the positioning of features on this map was made with the Mariner 10 pictures outlined above.



Index No.	FDS No.	Index No.	FDS No.	Index No.	FDS No.
1	001229	22	000215	43	000062
2	001223	23	000121	44	000056
3	000126	24	529129	45	000063
4	000195	25	000120	46	000064
5	000199	26	000119	47	000055
6	000191	27	000118	48	000065
7	000216	28	000123	49	000066
8	000187	29	000124	50	000067
9	000109	30	166913	51	000068
10	000217	31	000125	52	000069
11	000213	32	166827	53	000070
12	000113	33	166826	54	000071
13	000112	34	166906	55	000072
14	000111	35	166912	56	000050
15	000110	36	529126	57	000051
16	000114	37	166853	58	000052
17	000115	38	000057	59	000053
18	000116	39	000058	60	000054
19	000117	40	000059	61	166828
20	000218	41	000060		
21	000212	42	000061		

SUPPLEMENTAL SOURCE INDEX

The Mariner 10 pictures outlined above were used to provide additional detail on the map but were not used on the controlled mosaic.

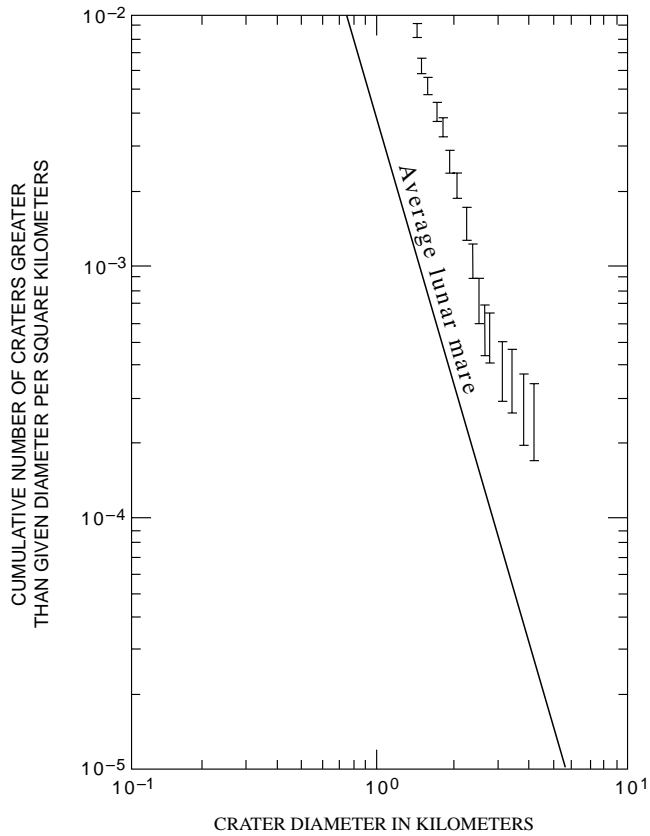


FIGURE 1.—Log-log cumulative crater-size-frequency distribution curve for smooth plains material (unit ps) within Tolstoj quadrangle. Position of average lunar-mare crater curve is added for reference only and does not imply absolute age difference. Bars represent standard error ($\sqrt{\frac{N}{A}}$, where N=cumulative number of craters and A=unit area).

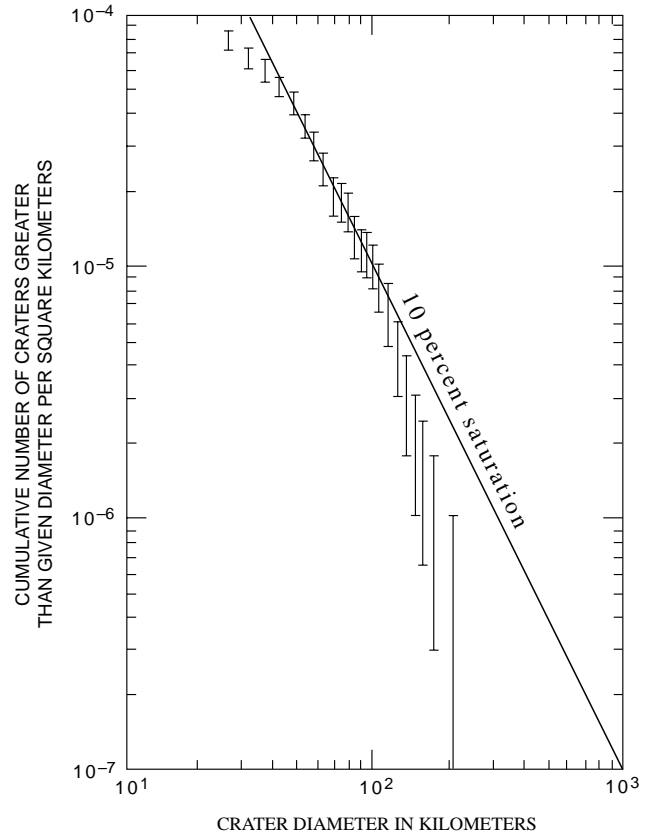


FIGURE 2.—Log-log cumulative crater-size-frequency distribution curve for heavily cratered terrain (unit pi and superposed $c_1 - c_5$ craters) within southeast half of Tolstoj quadrangle. Note fall away from 10-percent saturation surface (Gault, 1970) for craters with diameters smaller than 50 and larger than 90 km. Bars represent standard error (represent standard error ($\sqrt{\frac{N}{A}}$, where N = cumulative number of craters and A = unit area).

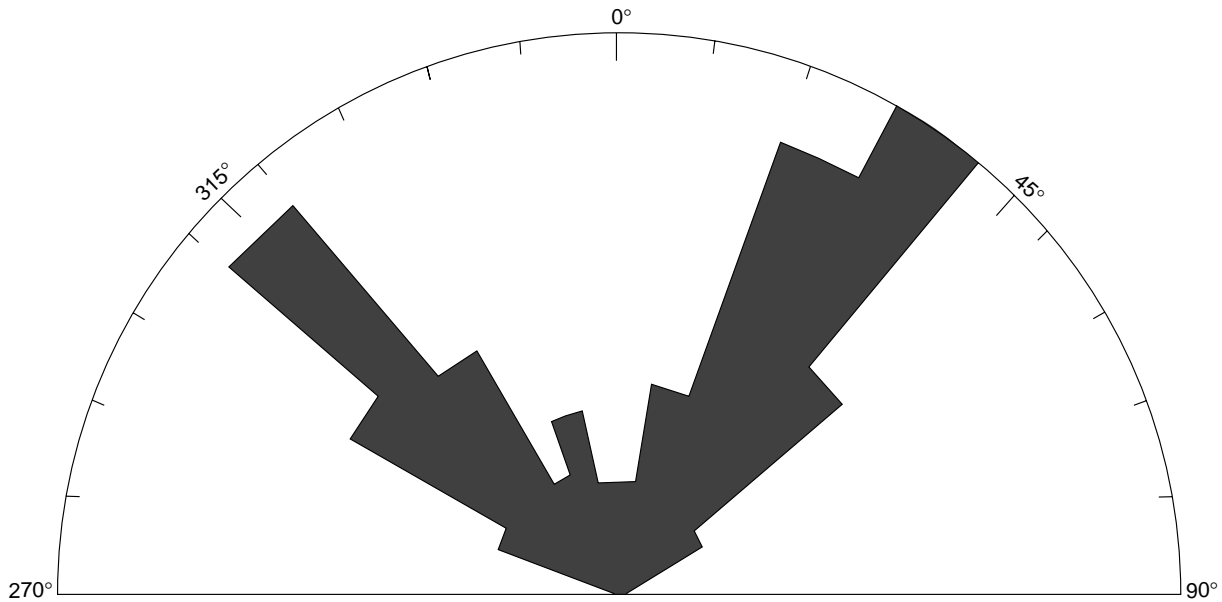


FIGURE 3.—Azimuth-frequency diagram showing azimuthal trends of linear features mapped within Tolstoj quadrangle. Length of sectors is proportional to number of linears.

NOTES ON BASE

This map sheet is one of a series covering that part of the surface of Mercury that was illuminated during the Mariner 10 encounters (Davies and Batson, 1975). The source of map data was the Mariner 10 television experiment (Murray, 1975).

ADOPTED FIGURE

The map projections are based on a sphere with a radius of 2439 km.

PROJECTION

The Mercator projection is used for this sheet, with a scale of 1:5,000,000 at the equator. Latitudes are based on the assumption that the spin axis of Mercury is perpendicular to the plane of the orbit. Longitudes are positive westwards in accordance with the usage of the International Astronomical Union (IAU, 1971). Meridians are numbered so that a reference crater named Hun Kal (lat -0.6°) is centered on long 20° (Murray and others, 1974; Davies and Batson, 1975).

CONTROL

Planimetric control is provided by photogrammetric triangulation using Mariner 10 pictures (Davies and Batson, 1975). Discrepancies between images in the base mosaic and computed control point positions appear to be less than 10 km.

MAPPING TECHNIQUES

Mapping techniques are similar to those described by Batson (1973a, 1973b). A mosaic was made with the pictures that had been digitally transformed to the Mercator projection. Shaded relief was copied from the mosaics and portrayed with uniform illumination with the sun to the west. Many Mariner 10 pictures besides those in the base mosaic were examined to improve the portrayal. The shading is not generalized, and may be interpreted with nearly photographic reliability (Inge, 1972; Inge and Bridges, 1976).

Shaded relief analysis and representation were made by Patricia M. Bridges.

NOMENCLATURE

All names on this sheet are approved by the International Astronomical Union (IAU, 1977).

H-8: Abbreviation for Mercury (Hermes) sheet number 8.
H 5M 0/180 G: Abbreviation for Mercury (Hermes) 1:5,000,000 series; center of sheet, lat 0° , long 180° ; geologic map, G.

REFERENCES

- Batson, R. M., 1973a, Cartographic products from the Mariner 9 mission: *Journal of Geophysical Research*, v. 78, no. 20, p. 4424–4435.
_____, 1973b, Television cartography: U. S. Geological Survey open-file report, no. 1960, 35 p.
Davies, M. E., and Batson, R. M., 1975, Surface coordinates and cartography of Mercury: *Journal of Geophysical Research*, v. 80, no. 17, p. 2417–2430.
Inge, J. L., 1972, Principles of lunar illustration: Aeronautical Chart and Information Center Reference Publication RP-72-1, 60 p.
Inge, J. L., and Bridges, P. M., 1976, Applied photointerpretation for airbrush cartography: *Photogrammetric Engineering and Remote Sensing*, v. 42, no. 6, p. 749–760.

International Astronomical Union, Commission 16, 1971, Physical study of planets and satellites, *in* Proceedings 14th General Assembly 1970: International Astronomical Union Transactions, v. 14B, p. 105–108.

_____ 1977, Physical study of planets and satellites, *in* Proceedings 16th General Assembly 1976, International Astronomical Union Transactions, v. 16B, p. 325, 331–336, 355–362.

Murray, B. C., 1975, The Mariner 10 pictures of Mercury: An overview: *Journal of Geophysical Research*, v. 80, no. 17, p. 2342–2344.

Murray, B. C., Belton, M. J. S., Danielson, G. E., Davies, M. E., Gault, D. E., Hapke, Bruce, O’Leary, Brian, Strom, R. G., Soumi, Verner, and Trask, Newell, 1974, Mercury’s surface: Preliminary description and interpretation from Mariner 10 pictures: *Science*, v. 185, no. 4146, p. 169–179.